

Ionic Strength and Electrostatic Effects in Biosorption of Protons

SILKE SCHIEWER AND
BOHUMIL VOLESKY*

Department of Chemical Engineering, McGill University,
3480 University Street, Montreal, Quebec, Canada H3A 2A7

New biosorbent materials are being developed for removal of heavy metals from effluents. This study investigates the effect of ionic strength on titrations of protonated *Sargassum* seaweed biomass and of alginate, a constituent molecule mainly responsible for the binding of cations in *Sargassum*. The results indicate a significant influence of electrostatic effects on the protonation behavior. The main objective of this work was to examine the capability of an adapted Donnan model to predict pH titrations of negatively charged biomass particles at different ionic strengths. The model, applicable for wider ranges of ionic strength and charge density in the biomass than other Donnan models in the recent literature, yielded good agreement of model predictions and experimental data. Swelling of the sorbent was found to increase with pH. While incorporating a linear relationship between swelling and pH improved the model predictions, it was not necessary in order to obtain reasonable predictions. The model required only three parameters: the total number of binding sites, the equilibrium constant ^{CH}K for proton binding, and only one additional parameter to model the influence of ionic strength, even when swelling was considered. Plots of the degree of dissociation versus (pH-pNa) as a criterion for the rigidity of the particle were found to be valid only under conditions where the concentration factor λ is high.

Introduction

Biosorption has been considered as an alternative technique of removing toxic heavy metals particularly from industrial effluents. Its cost-effectiveness makes it particularly attractive for this purpose. The performance of newly discovered biosorbent materials is being established in a series of recent studies (1). Since Na is present in many industrial wastewaters, it is useful to be able to estimate the extent to which Na interferes with the binding of heavy metal ions targeted by biosorption. Although it is known that sodium only binds weakly, through electrostatic attraction, a significant ionic strength effect may be observed if the Na concentration is varied over a wide range. Therefore, a mathematical model of the biosorption equilibrium should include the influence of ionic strength. Additionally, an electrostatic model accounting for ionic strength effects may eventually prove useful in the estimation of the extent to which electrostatic effects contribute to heavy metal sorption. Previous results from titrations of *Sargassum* biomass, which involved the measurement of the electrophoretic mobility of *Sargassum* (2), showed that *Sargassum* biomass bears a significant negative charge when the concentration (and therefore the binding) of protons or covalently bound divalent metal ions is low.

Obviously, this charge must lead to electrostatic attraction of cations. Until now, however, biosorption of metal ions has only been modeled using chemical binding constants (2), disregarding the effects of electrostatic attraction. The purpose of this work is to provide a model that includes ionic strength effects in biosorption modeling for charged and heterogeneous sorbent materials such as *Sargassum* biomass or alginic acid occurring as particles that are large in comparison to the double-layer thickness. The model should be suitable for a wide range of ionic strength values and also for conditions where the proton concentration significantly contributes to the magnitude of the ionic strength.

The simplest approach to modeling the influence of Na in the biosorption system consists of the introduction of a binding constant for Na, as done by Westall et al. (3) for humic acids (10–100 mM NaClO₄, pH 4.5–9.5, four discrete binding sites). The modeling results were close to the experimental data, but the range of the Na concentration employed in the experiments was small, and no general conclusions about the quality of the model can be made. The advantage of this approach is that binding of each species can easily be calculated using a multicomponent isotherm. Additionally, the Na binding constant can more easily be incorporated into computer programs for the calculation of chemical equilibria in aqueous solutions, such as MINEQL (4), than the respective terms for other models. One disadvantage is however that the Na binding constant is purely empirical and does not reflect the electrostatic nature of the Na binding.

A second possibility is the use of the Donnan model (5). An application of this approach for different charged polymers has been pioneered by Marinsky and co-workers (6), who established the use of Donnan models for organic polyelectrolytes including humic substances (7) and alginic acid (8). The latter contribution involves an estimation of the water uptake (swelling) using osmotic coefficients from the literature which, unfortunately, was not verified with experimental results. The relationships in different plots are discussed in terms of the Donnan model, but no model predictions of proton binding under different conditions were made. Thus the model fit for the data set could not be judged.

Only very recently has a Donnan model been used for the actual modeling of ionic strength effects in proton binding by humic acids ($I = 1-2000$ mM, pH = 3–10, two sites with affinity distribution) and bacterial cell walls ($I = 10-1000$ mM, pH 3–10, one site with affinity distribution) (9, 10). A linear decrease of the logarithm of the particle volume with the logarithm of the ionic strength was noted. The model was extended by Kinniburgh et al. (11) to also describe the binding of metal ions (Ca, Cd, Cu, Pb) to humic acid, employing the same swelling correlation. The model described the experimental data well. However, its disadvantage is that it requires a rather large number of fitting parameters.

Cabaniss (12) used Güntelberg activity coefficients to account for ionic strength effects on titrations of fulvic acids ($I = 5-100$ mM, pH = 5–8, five discrete binding sites), assuming that each fulvic acid molecule bears five negatively charged groups. This method is suited for rather small molecules and would not be appropriate for polyelectrolytes such as alginic acid or *Sargassum* biomass.

A model that is suitable for both oligo- and polyelectrolytes was used by Bartschat et al. (13) for modeling titrations ($I = 1-100$ mM, pH = 4–9, two binding sites) of humic acid molecules, which are assumed to be penetrable or impenetrable spheres of two size classes (assuming that the total charge is proportional to the volume of the sphere). An equation that relates the concentration factor λ to the charge

* Corresponding author e-mail: BOYA@CHEMENG.LAN.McGILL.CA; telephone: 514-398-4276; fax: 514-398-6678.

density per surface area (if impenetrable) or to the volumetric charge density (if penetrable), respectively, was used. For small λ the limiting case of simple charged molecules (Debye–Hückel or Tanford equations), and for large λ the limiting case of polyelectrolyte behavior (Gouy–Chapman or Donnan models) are approximated. The model showed good agreement with the experimental data of these authors. The advantage of this approach is its generality concerning the size of the molecule, which makes it particularly suited for oligoelectrolytes that show a behavior intermediate between simple ions and polyelectrolyte gels. For alginate or *Sargassum*, however, this feature is not necessary since they could be considered as true polyelectrolytes.

A Helmholtz model for the charged interface was used by Xue et al. (14) for the binding of protons and heavy metal ions to algal surfaces ($I = 10$ mM, pH = 3–9, one binding site). This model requires only one fitting parameter, the constant capacitance, for modeling the electrostatic effects. With a constant capacitance it is however not possible to predict ionic strength effects. When the cation binding at different ionic strengths is to be described, a new value for the capacitance has to be determined for each ionic strength.

Another model that needs few fitting parameters has been employed by Tipping (15, 16) for humic acids ($I = 1–1000$ mM, pH = 3–11, eight binding sites of two general types). The advantage of this model is its economical way of using relatively few fitting parameters for the prediction of a wide range of experimental conditions. Only one or two parameters are needed in order to predict λ (at the charged surface) at different ionic strengths. Unfortunately, however, the equation used by Tipping (16) for the relationship between the concentration factor λ and the ionic strength is an empirical one.

De Wit et al. (17) employed a Poisson–Boltzmann model for proton binding to humic substances ($I = 10–1000$ mM, pH = 2–10, one or two binding sites with affinity distribution). The advantages of this model are that it incorporates the effect of ionic strength on the concentration factor in a realistic manner and that it only needs one fitting parameter for electrostatic effects. Both for cylindrical and spherical impermeable particles, this fitting parameter is the particle radius. The assumption of small impermeable spheres or cylinders appears, however, not applicable to the large, penetrable particles investigated in the present study.

The work presented here makes an effort to represent the system in the simplest possible way that is physicochemically plausible and that gives reasonably low modeling errors, stating the assumptions and limitations of its validity. This way the observed behavior in the experiments and the fitting parameters can be interpreted in a meaningful way that contributes to the understanding of biosorption. In addition, the closer a model reflects the real processes, the better it can be expected to predict experimental conditions under which it was not originally derived. Purely empirical models usually fit for limited conditions only. In order to evaluate the validity of a model, a broad range of conditions has to be considered. Therefore, multiple independent variables were widely varied in this study (proton concentration, 5 orders of magnitude; Na concentration, about 4 orders of magnitude, two materials) in a range that produced pronounced variations of the dependent variable Hq . A high ratio between the number of experimental data points and the number of fitting parameters was achieved.

In order to select a suitable model for ionic strength effects, the properties of the biomass investigated have to be taken into account. Recent results indicated that the metal ion or proton binding sites in *Sargassum* biomass were predominantly the carboxyl groups of alginate and to a smaller extent also the sulfate groups of fucoxanthin (18). Since carboxyl groups are also one of the major functional groups in humic and fulvic acids (together with phenolic groups in humic acids),

some similarities in the polyelectrolyte properties of these materials can be expected. The main difference lies in the number of charges and the particle size. Since alginate is a macromolecule of about 80 monomers, each bearing one carboxyl group that may become negatively charged (19), the focus in this work is on polyelectrolyte (not oligoelectrolyte as for some fulvic acids) models. An additional difference is the particle size. For fulvic acids, 10 Å is a typical size (13). The double-layer thickness at low charge densities may therefore be larger than the fulvic acid diameter, so that the charge is not balanced within the particle. Algal particles on the other hand can be rather large. The average diameter for the *Sargassum* biomass particles employed in this study was about 1 mm. This is much larger than the double-layer thickness even at the lowest imaginable strength. Since ions can easily diffuse into the algal cell wall, it might therefore be appropriate to treat *Sargassum* biosorbent as a Donnan type gel where the charge is balanced in the particle. Consequently, Donnan models have been considered in this work. These will be more general than the one used by Marinsky and co-workers (7, 8), which included implicit assumptions that are not valid for the system in this study (see below).

This work focuses on a simple system involving two monovalent cations, only one of which binds covalently. The purpose is to compare experimental data on titrations of *Sargassum* and alginate at different ionic strengths with predictions by Donnan models. A further objective of this work was to evaluate whether swelling is relevant when *Sargassum* biomass is used and, if so, whether it is necessary to incorporate this in the modeling. Since swelling is expected to occur only to a small extent when divalent heavy metals are present (as this is the case in the application of biosorption for wastewater purification), only a preliminary investigation of the swelling behavior was made.

Materials and Methods

Materials. Beach-dried brown algal biomass of the genus *Sargassum*, collected in Natal, Brazil, was chopped manually and sieved. After washing with distilled de-ionized water, the biomass of the size fraction 0.5–1.7 mm was first washed twice in 1 N HCl (50 g of biomass/L) for protonation, then 10 times in the same volume of distilled de-ionized water, and finally dried in an oven at 60–80 °C. Protonation of the biomass was performed to eliminate any other exchangeable ions that were present on the raw biomass, thereby enabling the study of a simple sorption system, one involving only two cations. A stock solution of sodium alginate was prepared by dissolving 10 g of Na-alginate (Fisher) in 800 mL of distilled water.

Experiments. For the titrations, *Sargassum* biomass (0.1–0.5 g) or alginate (0.04–0.25 g dry weight) was contacted with 50 mL of sodium nitrate solution (concentrations below) in 125-mL Erlenmeyer flasks on a gyrotory shaker (New Brunswick Scientific, Model G2) at 2 Hz for 12 h. Different known amounts of HNO₃ or NaOH (0.1–1 M) were added to the samples in order to achieve different final pH values, which were measured (ORION Ionalyser Model 407A). The amounts of NaNO₃ initially added were for *Sargassum* as follows: 0 for the first series, 10 mM for the second series, 100 mM for the third series, and 1000 mM for the fourth series. For alginate, the initial NaNO₃ concentrations were as follows: 0 for the first and second series, 100 mM for the third series, and 1000 mM for the fourth series. The higher sorbent masses were generally applied at low pH values in order to avoid large experimental errors (20) and also for all data points of the second series.

In the swelling experiments, 0.25 or 0.5 g of *Sargassum* biomass and 10 mL of NaNO₃ solution (0–200 mM) were equilibrated overnight after adding some HCl or NaOH as required for pH adjustment. After measuring the pH, the

biomass was filtered off (using previously weighed Whatman No. 4 filter paper), weighed immediately, oven-dried at 60 °C, and weighed again after equilibrating at room atmosphere. Also for the alginate, the wet weight of the filtered gel and the dry weight after oven-drying were determined.

Model

General Equations. For all of the models used, the equations for the conservation of mass for the molecular species C (binding site, e.g., carboxyl), H , Na , and L (monovalent ligand, in this case NO_3) are

$${}^tC = C + CH \text{ (mmol/g)} \quad (1)$$

$${}^tH = (CH_i + [H_p]_i V_m) m + \frac{[H_{add}] V_{H,add} - [OH_{add}] V_{OH,add} + [H]_i V_i}{m} \text{ (mmol/g)} \quad (2)$$

$${}^tL = [L_p]_i V_m m + [H_{add}] V_{H,add} + [NaL]_i V_i = [L_p] V_m m + [L] V \text{ (mmol)} \quad (3)$$

where CH is the amount of protonated C sites, C is the amount of free *negatively charged* C sites, m is the mass of the sorbent, and V is the volume of the solution. The total amounts (as different molecular species in solid and liquid phase) of each component (C , H , L) are indicated by the superscript “ t ”. The subscript “ i ” denotes initial values, $[NaL]_i$ is, for example, the initial concentration of sodium salt in the solution before the biomass was added. The subscript “ add ” refers to the addition of acid (added volume $V_{H,add}$) or base for pH adjustment. $[H_p]_i$ and $[L_p]_i$ stand for excess acid initially present in the pores or cell of the biosorbent due to incomplete washing after protonation. For any ionic species “ X ”, the concentrations $[X]$ without subscript are the ones in the bulk solution, and $[X_p]$ is the average concentration of X in the cation binding volume of the particle. The specific volume that is active in cation binding (in this case the alginate layers of the cell wall) per mass of biosorbent is called V_m .

In the mass balance of protons (eq 2), the reaction for the dissociation of water $H_2O \rightleftharpoons H^+ + OH^-$ was not considered because it is negligible at $pH \leq 6$. In this study, the pH range studied was 2–6 since at lower pH the amount of metals bound in biosorption is very low and at higher pH precipitation of some metals may occur. Therefore, it is most important to study the protonation behavior of the biomass in this pH range. At pH 2–6, proton binding by brown algal biomass is mainly due to carboxyl groups; sulfate groups are deprotonated. Since sulfate groups in *Sargassum* biomass are only present in small quantities (18) they can be neglected unless biosorption at very low pH values ($pH < 2.5$) is studied. Consequently, only carboxyl and not sulfate groups as in the earlier work on biosorption with *Sargassum* (2) are considered. Phenolic groups that have a pK_a value of about 10 are protonated and do not play a role in either metal binding or acid-based reactions at pH 2–6. The term proton binding as used in this study refers to carboxyl groups only. The total proton binding by all groups of the biomass would of course be higher, but at $pH < 7$, the presence of phenolic groups only adds a constant amount to the total proton binding. The proton binding Hq is defined as the sum of the covalently (as CH) and electrostatically (as $[H_p] - [H]$) bound protons:

$${}^Hq = CH + ([H_p] - [H]) V_m \text{ (mmol/g)} \quad (4)$$

The final proton binding in the experiments can be calculated from eq 2:

$${}^Hq = CH_i + [H_p]_i V_m + \frac{[H_{add}] V_{H,add} - [OH_{add}] V_{OH,add} + [H]_i V_i - [H] V}{m} \text{ (mmol/g)} \quad (5)$$

The equations for charge neutrality in solution and in the particle or gel are for $[L] \gg [OH]$ (which is the case when $pH \leq 6$ as in this study):

$$[L] = [H] + [Na] \text{ (mmol/L)} \quad (6)$$

$$[H_p] + [Na_p] = [L_p] + C/V_m \text{ (mmol/g)} \quad (7)$$

where C is the number of charged groups in the biomass. The ionic strength in solution is defined as

$$I = 0.5 \sum z_j^2 [X_j] = 0.5 ([H] + [Na] + [L] + [OH]) \text{ (mmol/L)} \quad (8)$$

For $[OH] \ll [L]$, this can be simplified by substituting eq 6 into eq 8:

$$I = [L] \text{ (mmol/L)} \quad (9)$$

The apparent C site proton binding constant is

$${}^{CH}K_{app} = \frac{CH}{C[H]} \text{ (L/mmol)} \quad (10)$$

The degree of dissociation of the acidic group C is defined as

$$f = \frac{C}{{}^tC} = \frac{{}^tC - CH}{{}^tC} (-) \quad (11)$$

In the first approximation, assuming $CH \sim {}^Hq$, which is valid for ${}^tC[H] \ll {}^Hq I$ (see eq 19), this is equal to

$$f = \frac{C}{{}^tC} = \frac{{}^tC - {}^Hq}{{}^tC} (-) \quad (12)$$

Since no equation for calculating the experimentally obtained CH is mentioned in the available literature, it appears that most if not all other researchers assume that $CH \sim {}^Hq$, thus using eq 12. As pointed out in the section Variation of Apparent $p^{CH}K$, however, the assumption $CH \sim {}^Hq$ results in marked differences in the calculated ${}^{CH}K_{app}$ at low f , from which the intrinsic ${}^{CH}K$ is estimated. Therefore, this work makes a point in distinguishing between the amount of protons that are bound covalently (i.e., as CH) and electrostatically (i.e., as $[H_p] - [H]$). This requires the derivation of equations for CH (eq 19) and $[H_p]$ (eq 18) that reflect this situation. Substituting eq 11 in eq 10 and taking the logarithm yields

$$-p^{CH}K_{app} = pH + \log\left(\frac{1-f}{f}\right) (-) \quad (13)$$

The algorithm for the calculation of the variables Hq , CH , C , f , and $p^{CH}K_{app}$ from raw experimental data (i.e., final pH) is given in Figure 1a. Starting with the amount of protons bound (Hq), the other variables are calculated. The last terms to be evaluated are C (useful to know as a starting value for the model calculations, see Figure 1b) and $p^{CH}K_{app}$, which is plotted in some of the graphs.

Equations for Donnan Model (DO). The Donnan type model (DO) is based on an assumption that the intraparticle concentration may be different from the bulk concentration. The intraparticle concentration is assumed to be homogeneous throughout the reactive gel volume. The commonly

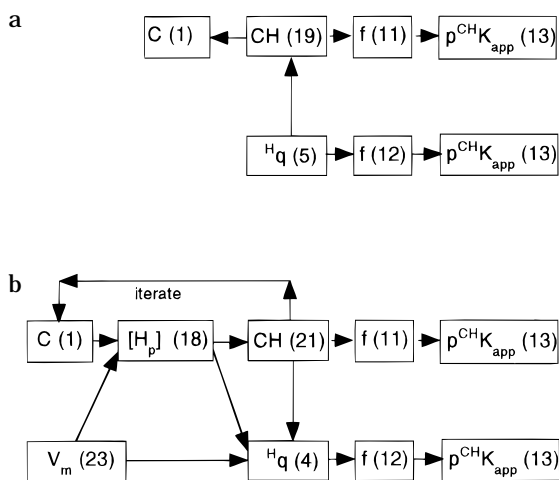


FIGURE 1. Calculation algorithm: (a) for experimentally determined variables and (b) for the Donnan model.

known equation for the concentration factor λ in an electrolytic gel according to the Donnan theory (5) is

$$\lambda^{z_x} = \frac{[X_p]}{[X]} \quad (-) \quad (14)$$

$$\frac{[Na_p]}{[Na]} = \frac{[H_p]}{[H]} \quad (-) \quad (15)$$

$$\frac{[H_p]}{[H]} = \frac{[L]}{[L_p]} \quad (-) \quad (16)$$

with $[X_p]$ being the concentration of any ionic species X with the charge z_x in the gel. Substituting $[Na_p]$ according to eq 7 into eq 15, solving the resulting equation for $[H_p]$ and replacing $[H] + [Na]$ with I (eqs 6 and 9) yields

$$\lambda = \frac{[H_p]}{[H]} = \frac{(C/V_m + [L_p])}{I} = \frac{C/V_m}{I} + \frac{1}{\lambda} \quad (-) \quad (17)$$

$[L_p]$ was expressed in terms of λ (14) after replacing I by L (eq 9). The recurring dimensionless group $C/(V_m I)$, which indicates the magnitude of intraparticle accumulation of ions as compared to the bulk ionic strength, will henceforth be called Q . The solution of the quadratic equation for $[H_p]$ that can be obtained from eq 17 is

$$\lambda = \frac{[H_p]}{[H]} = \frac{(C/V_m)}{2I} = \sqrt{\frac{(C/V_m)^2}{4I^2} + 1} = \frac{Q}{2} + \sqrt{\frac{Q^2}{4} + 1} \quad (-) \quad (18)$$

For conditions where $Q \gg 1$, eq 18 can be simplified as $\lambda = Q$. In the literature, this simple relationship between λ and Q has been obtained from eqs 15 and 7 by implicitly assuming high concentration factors λ or Q values (so that $[L_p] \sim [L] \ll C$ and $[Na] \gg [H]$ (such that $[Na] = I$ and $[Na_p] = C$) (6, 7). Compared to eq 18, this simplification yields errors of >10% for $Q < 3$, and the deviation reaches a factor of 2 or more for $Q < 0.7$. If, on the other hand, $Q \ll 1$, eq 18 can be simplified as $\lambda = 1 + 0.5Q$. This approximation yields a 10% discrepancy for $Q > 1.2$, and for high Q the maximum deviation can approach a factor of 2. A better approximation that is valid for high and low Q is $\lambda = Q + 1$. For this correlation, the error exceeds 10% for $0.3 < Q < 9$, but the maximum deviation is only 25%, which is reached at $Q = 1.5$.

In order to obtain a more general Donnan model that applies for any Q value and also under conditions where $[Na]$

$\gg [H]$ is not fulfilled, this work does not follow the simplifying equations but uses eq 18 instead. Only for calculating the amount of covalently bound protons from the experimental data, $\lambda = Q + 1$ is assumed in order to avoid iterative calculation of CH and $[H_p]$. This corresponds to setting $1/\lambda = 1$ in eq 17. Then eliminating C and $[H_p]$ using eqs 1 and 4 yields

$$CH = {}^H q \frac{I}{I - [H]} - {}^t C \frac{[H]}{I - [H]} \quad (\text{mmol/g}) \quad (19)$$

The above equation is useful in order to determine the CH value in the experiments, which is necessary for calculating f (eq 11) and thereby $p^{\text{CH}}K_{\text{app}}$ (eq 13). In most studies, it is assumed that $CH = {}^H q$. This is justified when ${}^H q$ or CH is the variable of interest because for all data points in this study $CH \geq 0.9 {}^H q$. When, however, a plot of $p^{\text{CH}}K_{\text{app}}$ versus f is used in order to extrapolate the intrinsic ${}^{\text{CH}}K$ (as done by ref 8), the values of $p^{\text{CH}}K_{\text{app}}$ at low f are of special importance for determining ${}^{\text{CH}}K$. At low f , however, even small differences between ${}^H q$ and CH can result in marked differences in f and therefore in $p^{\text{CH}}K_{\text{app}}$ because it is a function of $f/(1 - f)$ (eq 24). This is further discussed in the section Variation of Apparent $p^{\text{CH}}K$.

In the modeling, the intrinsic proton binding constant is defined as

$${}^{\text{CH}}K = \frac{CH}{C[H_p]} \quad (\text{L/mmol}) \quad (20)$$

Substituting C using eq 1 into eq 20, CH according to the Donnan model can be calculated as

$$CH = \frac{{}^t C {}^{\text{CH}}K [H_p]}{1 + {}^{\text{CH}}K [H_p]} \quad (\text{mmol/g}) \quad (21)$$

The relationship between the apparent and the intrinsic binding constant can be derived from eqs 10 and 20:

$${}^{\text{CH}}K_{\text{app}} = {}^{\text{CH}}K \frac{[H_p]}{[H]} = {}^{\text{CH}}K \lambda \quad (\text{L/mmol}) \quad (22)$$

Two versions of the Donnan model are considered in the following: one that assumes a rigid particle (DORI) and one that accounts for swelling (DOSW). The particle volume V_m is the fitting parameter that takes care of electrostatic effects for the rigid Donnan (DORI) model. Swelling changes the concentration of charged sites per volume and therefore also the concentrations of ions in the gel. It was observed (see section Physical Behavior of Biosorbents) that swelling of both *Sargassum* and alginate increased with pH and that there was no significant influence of I on swelling. Since one of the aims of his work is to keep the model as simple as possible, the following simple linear relationship between the specific particle volume and pH was assumed:

$$V_m = Y_V \text{ pH} \quad (\text{L/g}) \quad (23)$$

Y_V is a constant (for the DO model with swelling) that has to be determined by fitting the model to the experimental data for ${}^H q$. Since ${}^H q$ depends largely on ${}^{\text{CH}}K$ and $[H_p]$, which is in turn influenced by V_m , the latter variable represents the only one through which ionic strength effects can be accounted for. Although V_m is not independently determined but obtained by fitting Y_V to the binding data, the model reflects the physical reality in so far as a linear increase of V_m with pH was experimentally observed both for *Sargassum* and alginate (see section Physical Behavior of Biosorbents). When the model is to be used for other sorbent materials, the dependence of V_m from other parameters has to be established so that an appropriate correlation can be used. The method

of using the Donnan model in the study presented here, where an experimentally established correlation for the gel volume (eq 23) was used in order to predict the proton binding, was different from that by Lin (8), who used the binding data in order to calculate the gel volume for each data point.

The algorithm for the calculation of the proton binding and other variables is shown in Figure 1b. It is necessary to perform the calculations iteratively. It has proven a reliable, stable method to start the iteration by guessing that the concentration of free sites is equal to the experimentally determined value (eqs 1 and 19). In addition to C , V_m is the other starting value that, however, does not have to be calculated iteratively since it is constant for a given pH value. In each loop of the iteration, H_p , CH , and C have to be evaluated. When stable values are reached, the remaining variables Hq , f , and ultimately $p^{CH}K_{app}$ are calculated without further iteration.

Equations for the Plot of f versus (pH-pNa). In the earlier work of Marinsky (6, 7), it was recommended to plot $p^{CH}K_{app}$ versus (pH + pL) or versus pH. No influence of ionic strength should be noticed if, in the former case, the particle is rigid and permeable, or as in the latter case, if it is rigid and impermeable. As Cabaniss and Morel (21) pointed out, however, these plots are not reliable. They showed that it is more correct to plot f versus (pH-pNa). This type of a plot was then employed in the later work of Marinsky's research group (8). Neither of these authors give a mathematical justification of the use of this plot that indicates when it is valid. This will be undertaken in the present work. From eq 20 one can derive

$$-p^{CH}K = pH_p + \log\left(\frac{1-f}{f}\right) \quad (-) \quad (24)$$

For $Q \gg 1$ (that yields $[H_p] \gg [H]$) and substituting the corresponding simplification of eq 18, i.e., $[H_p] = [H]C/(V_m)$ yields

$$-p^{CH}K = pH - pI + p(C/V_m) + pf + p\left(\frac{f}{1-f}\right) = pH + p\left(\frac{f}{1-f}\right) + pQ \quad (-) \quad (25)$$

This equation is the justification for the plot of f versus (pH-pNa) if $[Na] \gg [H]$ (i.e., $[Na] \sim I$) is assumed: since $p^{CH}K$ and $p(C/V_m)$ are constant for a rigid particle, f is only a function of (pH-pNa), not a function of I . However, it would be more appropriate to plot f versus (pH-pI), which avoids making the additional assumption that $[Na] \gg [H]$. Furthermore, I is a more easily accessible variable. While Na has to be measured or calculated as a function of Hq , I can usually be assumed to be constant throughout the experiment and calculated from eq 3, assuming $[L_p] \sim L$.

If the opposite assumption is made, i.e., $Q \ll 1$ (or $[H] \sim [H_p]$), we obtain from eq 24 after subtracting pQ from the right-hand side and adding its equivalent, which is $p(C/V_m) + pf - pf$:

$$-p^{CH}K = pH + p\left(\frac{f}{1-f}\right) = pH - pI + p(C/V_m) + pf + p\left(\frac{f}{1-f}\right) - pQ \quad (-) \quad (26)$$

This means that compared to the above eq 25, the curves of f versus (pH-pNa) are shifted by pQ to the right. It now depends on which assumption is more appropriate: whether one or the other equation may be used. This will be discussed in a subsequent section, Modeling the Plot f versus (pH-pNa).

Experimental Results and Discussion

Titration Curves. Figure 2 shows the proton binding (Hq) by *Sargassum* biomass at different ionic strengths (I) of the

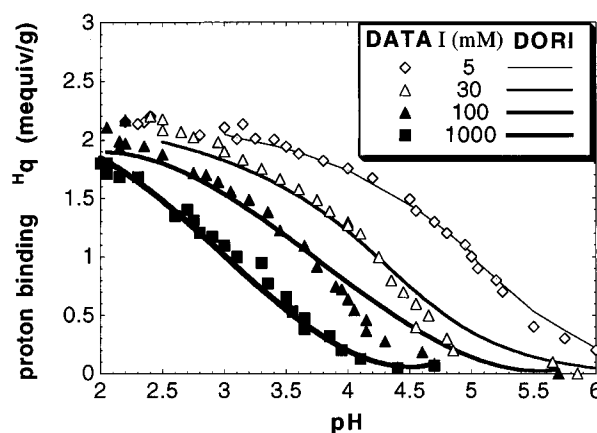


FIGURE 2. Titration of protonated *Sargassum* biomass at different ionic strengths. Experimental data and predictions of the Donnan model for rigid particles (DORI).

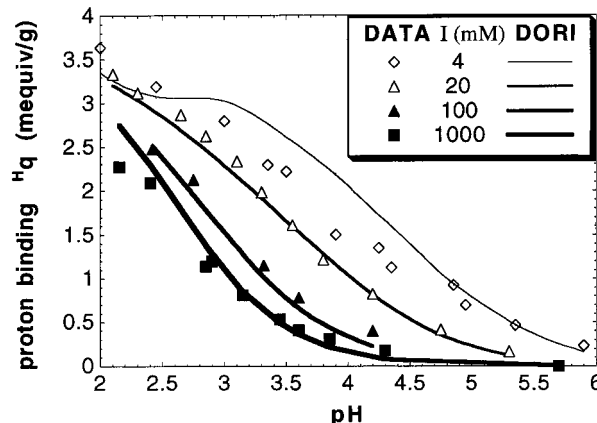


FIGURE 3. Titration of Na-alginate at different ionic strengths. Experimental data and predictions of the Donnan model for rigid particles (DORI).

solution as a function of pH. It should be noted that in this and in all other figures the I values that are given in the figure's legend refer to I at $f \sim 0.5$ of the respective series. Since different amounts of acid or base were added to each sample, the actual final ionic strength varies from point to point. The proton binding can be calculated from the mass balance for protons in eq 5 with $CH_i + [H_p]_i V_m = 2.6$ mmol/g. This value was chosen such that the inflection that signifies the end point of the titration of the carboxyl groups occurs at ${}^Hq = 0$. It can be noticed that the maximum proton binding and therefore the number of binding sites tC is equal to 2.1 mmol/g for any ionic strength. This means that 0.5 mmol/g of extra protons in the pores or in the cell would have been present due to incomplete washing (the values for tC , CH_i , and $[H_p]_i$ are further discussed in the section Determination of Model Parameters and Comparison with Experimental Results).

The apparent proton binding constant (${}^{CH}K_{app}$) changes drastically with ionic strength: while the $-p^{CH}K_{app}$ ($-p^{CH}K$ at half-dissociation of the acidic group) for low I is close to 5, it decreases to about 3 for high ionic strength. This corresponds to a change in the dissociation constants by a factor of 100. The observed shift in $p^{CH}K_{app}$ values is a common phenomenon in titrations of polyelectrolyte gels (7, 8, 15). The reason for this is that, due to electrostatic effects, the local proton concentration at the solid-solution interface $[H_s]$ is higher than the bulk concentration $[H]$. The half-dissociation for low ionic strength then does not really occur at pH 5 but at a local, lower pH (eq 22). The concentration factor λ , by which the local concentration exceeds the bulk concentration, decreases with increasing ionic strength (eq 18). Consequently, the electrostatic effects are low at high

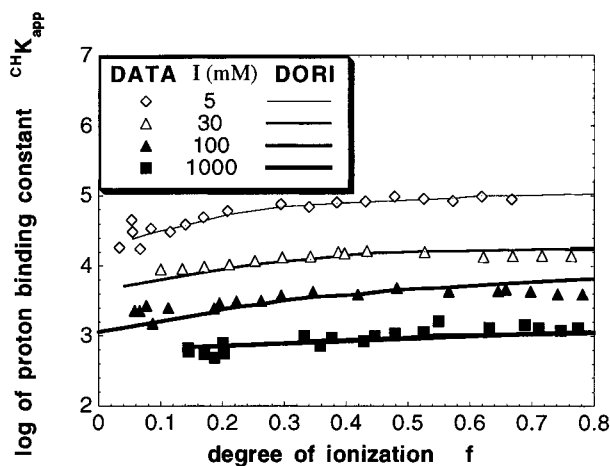


FIGURE 4. Variations of apparent pK for titration of protonated *Sargassum* biomass at different ionic strengths. Experimental data and predictions of the Donnan model for rigid particles (DORI).

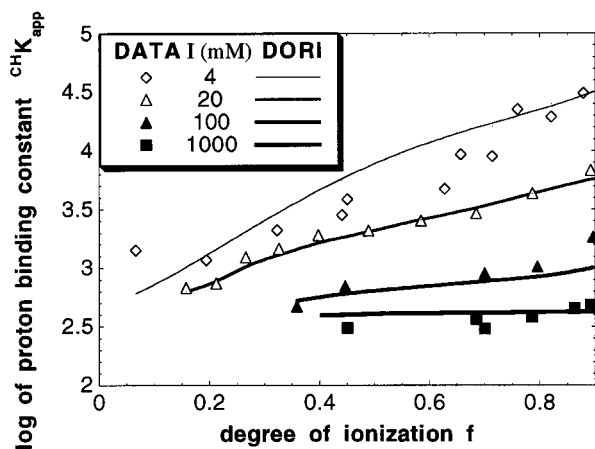


FIGURE 5. Variations of apparent pK for titration of Na-alginate at different ionic strengths. Experimental data and predictions of the Donnan model for rigid particles (DORI).

ionic strength such that the $p^{CH}K_{app}$ at high ionic strength approaches the intrinsic $p^{CH}K$.

The proton binding for alginate is shown in Figure 3. Equation 5 was evaluated with $CH_i + [H_p]_i V_m = 0$ because Na-alginate was used. Since the determination of proton accumulation becomes rather inaccurate at $pH < 2$, it is not possible to reliably calculate the proton binding at such low pH values. At $pH > 2$, however, the maximum proton binding is not yet achieved. Therefore, the total number of binding sites cannot be determined graphically. Consequently, it is also not possible to read the half-dissociation pH from the graph.

However, it is obvious that the $p^{CH}K$ values for alginate are generally lower than for *Sargassum*. Also, one can see that the curves for high and low ionic strength (the values of I are similar for both materials) are only separated by 1 pH unit as opposed to 2 pH units for *Sargassum*. This may indicate less pronounced electrostatic effects in the case of alginate.

Variation of Apparent $p^{CH}K$. Figures 4 and 5 show the influence of the degree of dissociation (f) and the ionic strength of $p^{CH}K_{app}$ for *Sargassum* and alginate, respectively. The apparent $p^{CH}K$ is calculated from eq 13 with the degree of dissociation, f , from eqs 11 or 12. The values of f obtained from these two methods do not differ widely, and consequently, the values for $p^{CH}K_{app}$ are also quite similar for most data points. At low f and low I , however, even a small difference in f has a significant effect on $p^{CH}K_{app}$. The $p^{CH}K_{app}$ values calculated with eq 12 are up to 0.25 unit higher than the ones calculated with eq 11 for the same data points (data

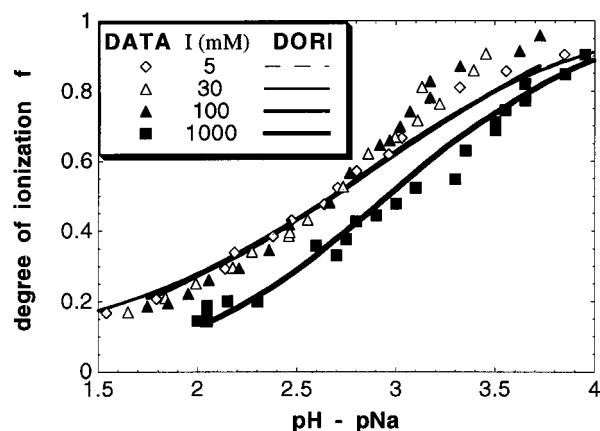


FIGURE 6. Plot of f versus $(pH - pNa)$ for titration of protonated *Sargassum* biomass at different ionic strengths. Experimental data and predictions of the Donnan model for rigid particles (DORI).

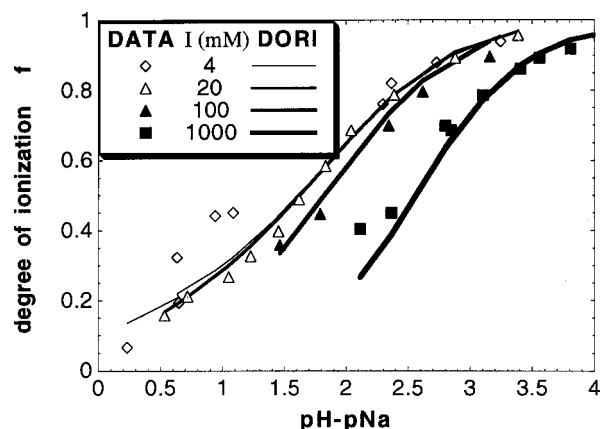


FIGURE 7. Plot of f versus $(pH - pNa)$ for titration of Na-alginate at different ionic strengths. Experimental data and predictions of the Donnan model for rigid particles (DORI).

not shown). As shown below, the value of $p^{CH}K_{app}$ for low f is of special importance for the extrapolation of the intrinsic $p^{CH}K_{app}$. Therefore, the calculation of f should be based on CH and not on H^+ if $p^{CH}K_{app}$ is of interest. As pointed out below, however, the extrapolation of $p^{CH}K$ from $p^{CH}K_{app}$ is not always reliable, although it has frequently been used in the past.

In general, it can be seen that the $p^{CH}K_{app}$ values for low I are generally higher and more strongly dependent on f . The apparent $p^{CH}K$ decreases with decreasing degree of dissociation. As f goes toward zero, $-p^{CH}K_{app}$ (using f from eq 11) for the alginate approaches a value of about 2.6 for any ionic strength, while for *Sargassum* $-p^{CH}K_{app} = 3 - 4.5$ (depending on the ionic strength) is approached. The decrease of $p^{CH}K_{app}$ with decreasing f can be explained as the result of a decreasing concentration factor with a decreasing charge (eqs 22 and 18) when the degree of dissociation decreases. For increasing ionic strength or decreasing degree of dissociation, the concentration factor approaches unity since the term Q in eq 18 approaches 0. Consequently, the $p^{CH}K_{app}$ value is expected to approach the intrinsic $p^{CH}K$ under these conditions, and electrostatic effects are no longer relevant. The fact that the curves for *Sargassum* do not appear to converge toward a common value for all ionic strengths may be due to the fact that electrostatic effects are stronger in *Sargassum* such that they only become negligible at very low degrees of dissociation for which no data points exist. It is therefore preferable to determine the intrinsic $p^{CH}K$ by nonlinear fitting to the proton binding data (as done in this study) rather than to extrapolate it from a plot of $p^{CH}K_{app}$ versus f (as done by Lin (8)).

Plot of f versus $(pH - pNa)$. According to Cabaniss (21), a plot of the degree of dissociation versus $(pH - pNa)$ reveals

whether a polyelectrolyte gel is rigid or flexible (eq 25): for a given degree of dissociation, the value of $(\text{pH} - \text{pNa})$ should not vary with ionic strength if the gel is rigid whereas it may vary for flexible gels. Figures 6 and 7 show this type of plot for *Sargassum* and alginate, respectively. It appears that *Sargassum* behaves as a rigid particle since little ionic strength effect is observed in this plot. However for $I = 1000$, there seems to be some flexibility of the particle. In contrast, alginate obviously swells since the curves for different ionic strength deviate strongly from each other. This result is intuitively appealing because the fact that alginate swells is known from the literature (8, 22), and less swelling can be expected for *Sargassum* because its alginate is constrained in the cellulose matrix of the cell wall.

Physical Behavior of Biosorbents. Swelling experiments were performed in order to test the hypothesis that alginate is flexible while *Sargassum* is not and also to obtain information about the relationship between swelling and experimental conditions such as pH and ionic strength. The ratio between the wet weight of the biomass after swelling and its dry weight after swelling and oven-drying was calculated. The ratio was proportional to the specific total volume tV_m of the biomass. The specific total volume tV_m increased from 5 to 10 mL/g when the pH was raised from 2 to 4.5. The regression coefficient for a linear correlation between tV_m and pH was $R = 0.88$ (data not shown). No influence of ionic strength was noticeable ($R = 0.19$, data not shown). Since the specific total volume changed by as much as a factor of 2, swelling appears to be relevant in *Sargassum*. It has to be mentioned, however, that only volume changes in the volume V_m that is active in proton binding (i.e., the alginate zone of the biomass) are of importance for the protonation behavior. These volume changes may not necessarily correspond to overall volume changes of the particle. Therefore, the results from the swelling experiments cannot be used for modeling purposes in a quantitative way. That means that the parameter Y_V (eq 23) still has to be determined by fitting to the experimental binding data while the qualitative dependency of V_m from pH, which lead to the formulation of eq 23, was experimentally determined.

For alginate, the amount of mass recovered decreased more significantly with increasing pH (no data shown) as compared with *Sargassum* biomass. Already at pH 3 very little alginate was recovered. This can be explained by the fact that sodium alginate is soluble. For the remaining recovered mass, the ratio between wet gel mass and dry mass was calculated analogous to *Sargassum*. The specific volume V_m increased from about 20 to about 200 mL/g when pH rose from 1.5 to 3.5 (data not shown). The regression coefficient for a linear correlation between tV_m and pH was $R = 0.81$. Little influence of ionic strength was noticeable ($R = 0.45$, data not shown). Although these values are not to be taken quantitatively (because it is difficult to estimate how much excess liquid remained in the gel), from the measured volume change by a factor of 10 it can be concluded that alginate swelling strongly increases with pH. This corresponds to experimental results of Moe et al. (22) for alginate swelling where the volume was observed to increase with pH. Whether alginate swelling in this study also increased with decreasing salt concentration as observed by Moe et al. (22) was not clearly discernible.

Determination of Model Parameters and Comparison with Experimental Results. It was established that three parameters were necessary and sufficient. Apart from the total number of binding sites tC and the equilibrium constant for proton binding ${}^{\text{CH}}K$, which are already necessary for modeling a single titration curve, only one more parameter was necessary in order to account for the effect of ionic strength. The third parameter for the DORI and DOSW

models were V_m and Y_V , respectively. Attempts at using instead of $V_m = Y_V \text{pH}$ a swelling correlation $V_m = \text{const} + Y_V \text{pH}$, which involves one more fitting parameter, were not successful: the optimization procedure (for which the computer program MATLAB 4.2c was used in order to minimize the deviations between modeled and experimentally determined ${}^{\text{H}}q$) did not yield stable results.

For *Sargassum* biomass, the value ${}^tC = 2.1$ mmol/g for the total number of binding sites was read directly from Figure 2, after assuming that all sites were initially occupied by protons and choosing $[\text{H}_p]_i V_m = 0.5$ mmol/g so that the ${}^{\text{H}}q$ at high f approaches zero where an inflection of the curves occurs so that the proton binding does not change much with pH.

Theoretically, one might expect that for low ionic strength the electrostatic binding of protons could be strong enough to balance most of the negative charge in the biomass so that the proton binding could still be significant, e.g., at pH 6. In reality, however, the amount of Na added for pH adjustment is so high that even when no NaNO_3 was added (i.e., the series with the lowest I) the electrostatic proton binding is low because $[\text{H}] \ll I$ for $\text{pH} > 4$. Therefore, the proton binding in the experiments for low I strongly decreases between pH 3.5 and pH 5.5.

The value of $[\text{H}_p]_i V_m = 0.5$ mmol/g corresponds to the amount of protons released when the protonated biomass is equilibrated in distilled water where no exchangeable ions are present (0.46 mmol/g was the average of four samples). Since the charge of the biomass must remain balanced by counterions, the protons released must have been excess HCl from the protonation (that had not been removed during previous washing with distilled water) because no other cations were present in the system (complete protonation).

The value for ${}^tC = 2.1$ mmol/g is in accordance with previous results for *Sargassum* biosorption (2). tC for the alginate (see Table 1) was obtained from the fitting procedure. When the obtained value is compared with 4.74 mmol/g, which should be the theoretical number of binding sites in pure Na-alginate, it appears that about 20 wt % of the material used may have been not alginate but, for example, excess sodium salt. This seems to be a reasonable magnitude.

For the models, the $\text{p}^{\text{CH}}K$ values were about equal to the pH of half-dissociation for high ionic strength (Figures 2 and 3). This means that one could obtain the intrinsic $\text{p}^{\text{CH}}K$ easily by reading it from the titration curve at $I = 1000$ mM. Also, it can be possible to obtain the intrinsic $\text{p}^{\text{CH}}K$ by extrapolating $\text{p}^{\text{CH}}K_{\text{app}}$ to $f = 0$ in Figures 4 and 5. For alginate at $I = 20$ or 100 mM, the lines of $\text{p}^{\text{CH}}K_{\text{app}}$ for f approaching zero are close to the fitted value of 2.6–2.7. The value of $\text{p}^{\text{CH}}K$ determined by Lin et al. (8) for alginate using the Donnan model was 2.95. It has to be mentioned, however, that this is only a rough and somewhat arbitrary estimate since no points for $f < 0.2$ were given by this author. For *Sargassum* the fitted value of about 3 is between the $\text{p}^{\text{CH}}K_{\text{app}}$ values for f approaching 0 at $I = 100$ (~3.2) and at $I = 1000$ mM (~2.8), but it was not possible to extrapolate the intrinsic $\text{p}^{\text{CH}}K$ from data at lower I .

For both *Sargassum* and alginate, the volume in the DORI model corresponded to that in the DOSW model at high pH, which is reasonable because electrostatic effects are especially noticeable at high pH (i.e., at high pH the volume has the strongest effect on binding). The model predicts that both *Sargassum* and alginate swell by a factor of 2 when the pH rises from pH 2 to pH 4. This corresponds to the swelling behavior observed in *Sargassum*, but it is less pronounced than the swelling observed in alginate. While on the one hand, additional water retained after filtering may produce seemingly high values of V_m in the experiments, one may, on the other hand, consider using a different swelling correlation, e.g., one where V_m is proportional to $(\text{pH})^2$. When the absolute values of V_m in the model and in the experiment are compared,

TABLE 1. Model Parameters and Absolute Mean Square Errors of the Model in Percent of tC

	DORI model		DOSW model	
	<i>Sargassum</i>	alginate	<i>Sargassum</i>	alginate
	Model Parameters			
tC	2.1	3.7	2.1	3.6
$-p^{CHK}$	2.8	2.58	2.65	2.6
3rd parameter	$V_m = 1.4$ mL/g	$V_m = 17$ mL/g	$Y_v = 0.22$ mL/g	$Y_v = 4.2$ mL/g
	Error at Different f^a			
5 mM	3.0	8.9	2.3	8.3
30 mM	6.1	2.7	5.3	2.5
100 mM	6.8	3.7	6.8	3.2
1000 mM	3.7	5.1	3.6	4.8
av^b	4.9	5.1	4.5	4.7
av^b error for both sorbents	5.0		4.6	

^a Since f varies from point to point, the value at $f = 0.5$ is given here. ^b Mean deviation of the errors in the eight series from the average error for all eight series.

it is obvious that the specific volume determined experimentally from the fraction of wet/dry weight after swelling is consistently larger than the one from the model (by a factor of about 6 for alginate and by a factor of about 4 for *Sargassum* for an average value at $f = 0.5$). This could be explained, for example, by assuming that only a fraction of the particle volume is active in proton binding. This assumption certainly does not hold for alginate because all of it should be an active volume. Also for *Sargassum*, it can be expected that the alginate volume makes up more than one-quarter of the total volume since it constitutes about 50% of the mass. Therefore, this can be at best only a partial explanation. Another plausible explanation could be that the concentration at the binding site is indeed higher than the average concentration in the particle but that the Donnan model, because it cannot predict a concentration profile, predicts a "step function" of the concentration instead. This would assume that all the ions that are accumulated in the particle because of electrostatic effects are concentrated in a smaller volume where the concentration is equal to the one at the interface.

Modeling Titration Curves. The model fits are compared in Table 1. The mean square of the absolute deviations (mmol/g) of the model from the experimental data is for convenience expressed in percent of the total binding capacity tC . The DOSW model has slightly smaller average errors (average error 4.6%) than the DORI model (4.9%), which has the advantage of being simpler. In order to avoid too many or too cluttered figures, only the modeling using the DORI model is presented in the figures. This model was chosen for the figures because it is the simpler one. The DORI model fits the data in Figures 2 and 3 well, only for the lowest ionic strength in the titration of alginate are there larger deviations (same applies for Figure 5). These are probably due to the fact that swelling is neglected because the model fit especially for this series improves significantly when the DOSW model is used (see Table 1).

Modeling the Variation of Apparent p^{CHK} . For both models the apparent p^{CHK} at $I = 1000$ mM is approximately constant and equal to the intrinsic one. For *Sargassum*, extrapolation of the intrinsic p^{CHK} from curves of p^{CHK}_{app} for f approaching zero is difficult at a moderate ionic strength. This may be due to a continuing importance of electrostatic effects even at low degrees of ionization, which may be caused either by a higher charge density (i.e., lower Y_v) or by the presence of additional acidic groups that are still ionized at low pH (e.g., sulfate groups). However, since the data are reasonably well described by the model predictions, which are based on the assumption that only one binding site exists, one can conclude that the observation that even at low f the experimental $p^{CHK}_{app} > p^{CHK}$ does not necessarily indicate the presence of a second site.

Modeling the Plot of f versus (pH-pNa). For *Sargassum*, the two models predict the data points well (DORI modeling shown in Figure 6). The curves for $I \leq 100$ are very close together, only the one for $I = 1000$ is shifted toward the right. For alginate, the models underpredict f at low (pH-pNa) values, but otherwise they are also appropriate (DORI modeling shown in Figure 7).

An interesting observation is that even the rigid Donnan model (DORI) predicts an effect of ionic strength in this type of plot. This is contrary to the theory (8, 21) according to which the curves for all I values should coincide for rigid polymers. A closer look at the underlying equation (25) reveals that the assumption that the intraparticle accumulation of H or Na is much larger than the bulk concentration (Q or $\lambda \gg 1$) does not hold. The values of Q as predicted by the DORI model for $I = 10, 100, \text{ or } 1000$ mM, respectively, are 4.0, 1.1, and 0.21 for pH 2 and 39, 9.3, and 1.4 for pH 4. It can be seen from these values that the assumption (i.e., $Q \gg 1$) for the present data set is only valid at low ionic strengths and high pH. Both H_p and H are of a comparable magnitude already for $I = 100$. For $I = 1000$ and low pH, the relationship is even reversed: $Q \ll 1$, i.e., the average intraparticle concentration $[H_p]$ is similar to the bulk concentration $[H]$. Under this opposite limiting case, it can be expected that the curves generated by eq 26 shift by pQ to the right as compared to the opposite assumption (eq 25).

For most data points the real behavior is, therefore, intermediate between the two limiting cases, and a smaller shift to the right occurs. This shift is the largest for high I values and low f (i.e., low pH). For low I values the curves are closer to the limiting case considered by other authors. The use of this plot as a criterion for rigidity is thus not recommended unless it is known that the criterion $\lambda \gg 1$ is fulfilled. Unfortunately, no evidence for fulfilling these conditions was given in most publications where this plot has been used, and neither has this assumption been explicitly stated.

Another implication of the fact that for most conditions neither $Q \gg 1$ nor $Q \ll 1$ is fulfilled is that the simplifications of eq 18 are not valid. Lin and Marinsky (8) used the approximation $\lambda = Q$, which predicts at high I markedly different values for $[H_p]$ than eq 18, resulting in different values for H_q . For example, at pH 2 and $Q = 0.5$, the correct value for $[H_p]$ (eq 18) is ~ 2.5 times higher than the one according to the simplification, for which $[H_p]$ is even smaller than $[H]$. The resulting reduction in the calculated proton binding is $\sim 15\%$.

Acknowledgments

The DAAD (German Academic Exchange Service) HSP2 scholarship for S. Schiewer is gratefully acknowledged.

Glossary

Model Abbreviations

DORI	Donnan model assuming rigid particle
DOSW	Donnan model assuming particle swelling

Variables

tC	total amount of binding sites C (mequiv/g)
f	degree of ionization
I	ionic strength (mmol/L)
${}^{CH}K$	equilibrium constant of proton binding (formation) (L/mmol)
m	dry weight of biomass (g)
pK, pX	$-\log$ of K (in L/mol) or of concentration (in mol/L)
Q	$= C/(V_m I)$ dimensionless factor
Hq	proton binding (covalent and electrostatic) (mequiv/g)
V	volume of solution (L)
V_m	specific particle volume per dry weight (L/g)
Y_V	fitting parameter for V_m (L/g)
z_X	charge of species X
λ	concentration factor
$[X]$	concentration (of molecular species X) (mmol/L)

Molecular Species

C	free binding sites
CH	binding site occupied by H
H	protons
L	ligand
Na	sodium
X	any ionic species

Indices

add	added
app	apparent
H	of acid
i	initial

p	average in particle
OH	of base
t	total

Literature Cited

- (1) Volesky, B.; Holan, Z. R. *Biotechnol. Prog.* **1995**, *11*, 235–250.
- (2) Schiewer, S.; Volesky, B. *Environ. Sci. Technol.* **1995**, *29*, 3049–3058.
- (3) Westall, J. C.; Jones, J. D.; Turner, G. D.; Zachara, J. M. *Environ. Sci. Technol.* **1995**, *29*, 951–959.
- (4) Schecher, W. D. *MINEQL+: A Chemical Equilibrium Program for Personal Computers, Users Manual Version 2.22*; Environmental Research Software, Inc.: Hallowell, ME, 1991.
- (5) Donnan, F. G. *Z. Elektroch.* **1911**, *17*, 572–581.
- (6) Marinsky, J. A. In *Aquatic Surface Chemistry*; Stumm, W., Ed.; Wiley Interscience: New York, 1987; pp 49–81.
- (7) Marinsky, J. A.; Ephraim, J. *Environ. Sci. Technol.* **1986**, *20*, 349–354.
- (8) Lin, F. G.; Marinsky, J. A. *React. Polym.* **1993**, *19*, 27–45.
- (9) Benedetti, M. F.; van Riemsdijk, W. H.; Koopal, L. K. *Environ. Sci. Technol.* **1996**, *30*, 1805–1813.
- (10) Plette, A. C. C.; van Riemsdijk, W. H.; Benedetti, M. F.; van der Wal, A. *J. Colloid Interface Sci.* **1995**, *173*, 354–363.
- (11) Kinniburgh, D. G.; Milne, C. J.; Benedetti, M. F.; Pinheiro, J. P.; Filius, J.; Koopal, L. K.; van Riemsdijk, W. H. *Environ. Sci. Technol.* **1996**, *30*, 1687–1698.
- (12) Cabaniss, S. E.; Shuman, M. S. *Geochim. Cosmochim. Acta* **1988**, *52*, 185–193.
- (13) Bartschat, B. M.; Cabaniss, S. E.; Morel, F. M. M. *Environ. Sci. Technol.* **1992**, *26*, 284–294.
- (14) Xue, H.-B.; Stumm, W.; Sigg, L. *Water Res.* **1988**, *22*, 917–926.
- (15) Tipping, E.; Backes, C. A.; Hurley, M. A. *Water Res.* **1988**, *22*, 597–611.
- (16) Tipping, E. *Environ. Sci. Technol.* **1993**, *27*, 520–529.
- (17) de Wit, J. C. M.; van Riemsdijk, W. H.; Koopal, L. K. *Environ. Sci. Technol.* **1993**, *27*, 2005–2014.
- (18) Fourest, E.; Volesky, B. *Environ. Sci. Technol.* **1996**, *30*, 277–282.
- (19) Chapman, V. J. *Seaweeds and Their Uses*; Chapman & Hall: London, U.K., 1980; pp 194–240.
- (20) Schiewer, S.; Volesky, B. *Biotechnol. Tech.* **1995**, *9*, 843–848.
- (21) Cabaniss, S. E.; Morel, F. M. M. *Environ. Sci. Technol.* **1989**, *23*, 746–747.
- (22) Moe, S. T.; Skjak-Braek, G.; Elgsaeter, A.; Smidsrod, O. *Macromolecules* **1993**, *26*, 3589–3597.

Received for review May 17, 1996. Revised manuscript received February 3, 1997. Accepted February 12, 1997.[®]

ES960434N

[®] Abstract published in *Advance ACS Abstracts*, April 15, 1997.